The dengue virus NS2B-NS3 protease retains the closed conformation in the complex with BPTI

Wan-Na Chen[a], Karin V. Loscha[a], Christoph Nitsche[b], Bim Graham[c], Gottfried Otting[a,*]

[a] Australian National University, Research School of Chemistry, Canberra, ACT 0200, Australia

[b] Medicinal Chemistry, Institute of Pharmacy and Molecular Biotechnology, Heidelberg University, Im Neuenheimer Feld 364, 69120 Heidelberg, Germany

[c] Medicinal Chemistry and Drug Action, Monash Institute of Pharmaceutical Sciences, Parkville, VIC 3052, Australia

* Corresponding author.

Fax: +61 (0)2 61250750

E-mail address: gottfried.otting@anu.edu.au (G. Otting).

Abstract

The C-terminal β-hairpin of NS2B (NS2Bc) in the dengue virus NS2B-NS3 protease is required for full enzymatic activity. In crystal structures without inhibitor and in the complex with bovine pancreatic trypsin inhibitor (BPTI), NS2Bc is displaced from the active site. In contrast, nuclear magnetic resonance (NMR) studies in solution only ever showed NS2Bc in the enzymatically active closed conformation. Here we demonstrate by pseudocontact shifts from a lanthanide tag that NS2Bc remains in the closed conformation also in the complex with BPTI. Therefore, the closed conformation is the best template for drug discovery.

Keywords: bovine pancreatic trypsin inhibitor; dengue virus protease; lanthanide tag; NMR spectroscopy; pseudocontact shift

Abbreviations: dengue virus (DENV); West Nile virus (WNV); dengue virus protease (DENpro); pseudocontact shift (PCS); bovine pancreatic trypsin inhibitor (BPTI); disulfide bond isomerase C (DsbC)

Highlights:

- Dengue virus NS2B-NS3 protease assumes closed conformation in complex with BPTI
- Solution conformation is different from crystal structure
- There is no evidence for significant population of open conformations in solution
- The closed conformation is the best template for rational drug discovery

1. Introduction

Dengue virus (DENV) is the most important mosquito-borne pathogen in terms of human suffering and cost, with a high rate of hospitalization and potentially deadly outcome [1]. There are four different closely related serotypes (DENV-1–DENV-4). To date, no approved vaccine or drug is available for any of them, but an established drug target is presented by the NS2B-NS3 protease (NS2B-NS3pro) formed from segments of the non-structural virus proteins NS2B and NS3 [2,3]. For a long time, however, development of an inhibitor of NS2B-NS3pro has been hampered by difficulties to ascertain the correct structure of the protein.

The first crystal structure of NS2B-NS3pro, determined for a construct from DENV-2, displayed an open conformation in which the C-terminal segment of NS2B (NS2Bc; residues 66*–95*; throughout this text, residue numbers of NS2B are identified by asterisks) was located far from the active site in an inactive conformation (Fig. 1) [4]. Subsequent NMR studies showed, however, that the protease assumes a closed conformation in solution, where NS2Bc lines the substrate binding site [5–7], in complete analogy to the structure of the related West Nile virus protease [4,8,9]. A crystal structure of NS2B-NS3pro from DENV-3 in complex with a peptide inhibitor confirmed the closed conformation [10], but the same protein in complex with the high-affinity (K_i = 26 nM [11]) trypsin inhibitor BPTI lacked any electron density for NS2Bc, indicating once again an open conformation [10].

In the absence of firm information about the correct target structure in solution, computational ligand binding studies targeting the active site used either closed or open conformations of the NS2B-NS3 protease [12-28]. Unfortunately, the actual three-dimensional (3D) structure in solution cannot readily be determined by conventional

NMR methods due to poor spectral resolution, line broadening by conformational exchange and limited protein stability. In the case of the NS2B-NS3pro complex with BPTI, its high molecular weight (35 kDa) further impedes NMR analysis.

Here we show that, in solution, the closed conformation prevails also in the presence of BPTI. This result was obtained by measuring pseudocontact shifts (PCS) of ^{15}N-HSQC cross-peaks of backbone amides in uniformly and selectively ^{15}N-labelled samples with a paramagnetic lanthanide tag attached to NS3pro. The PCSs provide a clear picture of the binding mode of BPTI at the active site and of the location of the β-hairpin of NS2Bc.

2. Materials and Methods

2.1 Expression plasmids

The DENV-2 NS2B-NS3 protease was produced without a covalent link between NS2B and NS3pro, using a previously described construct in which NS2B is separated from NS3pro by the natural protease recognition sequence EVKKQR [7]. The entire construct consists of the T7 gene 10 N-terminal peptide MASMTG followed by a two-residue cloning artifact (Leu-Glu), 47 residues from NS2B, the cleavage sequence EVKKQR, 185 residues from NS3pro and a C-terminal His_6-tag. The gene was inserted into the pETMCSI expression vector [29] and the plasmid was transformed into the *E. coli* strain Rosetta::λDE3/pRARE. An additional construct contained the single-cysteine mutation S68C in NS3pro for subsequent ligation with lanthanide tags [5]. The nucleotide sequence of BPTI [30] was also subcloned into the pETMCSI T7 expression vector and transformed into the *E. coli* strain TOP10 (Life Technologies, Carlsbad, CA, USA). The N-terminus was preceded by a His_6-tag followed by the tobacco etch virus (TEV) protease cleavage sequence ENLYFQG.

2.2. Protein sample preparation

Uniformly and selectively ^{15}N-labelled samples of the protease were made by high-cell density *in vivo* expression [31] and cell-free synthesis [32–34], respectively, and purified as described previously [7]. BPTI samples selectively labelled with ^{15}N-labelled Ala, Arg, Lys, Thr, Leu, Phe and Ile (Cambridge Isotope Laboratories, Andover, MA, USA; ISOTEC, St. Louis, MO, USA) were prepared by cell-free synthesis at 30 ^{o}C overnight following a published protocol that includes His_6-tagged disulfide bond isomerase C (DsbC) to catalyze correct disulfide bond formation [30]. The reaction volume was 1 mL in a dialysis tube of Spectra/Por 2 (MWCO: 12-14 kDa) suspended in 10 mL outer buffer. The protein was purified by diluting the supernatant of the cell-free reaction with 2 times buffer A (50 mM HEPES, pH 7.5, 300 mM NaCl), loading the mixture onto a Ni-NTA agarose spin column (Qiagen, Hilden, Germany), washing with buffer A plus 30 mM

imidazole and eluting with buffer A plus 300 mM imidazole. BPTI was separated from DsbC by a spin column containing SP-650M resin (TOSOH, Minato, Japan), using buffer B (50 mM HEPES, pH 8.0) with 50 mM NaCl for loading, buffer B with 100 mM NaCl for washing and buffer B with 1 M NaCl for elution. All purified proteins were exchanged into NMR buffer (20 mM MES, pH 6.5, 50 mM NaCl, 10% D_2O). Protein concentrations were determined by their UV absorbance at 280 nm.

Samples of the protease–BPTI complex were prepared either with ^{15}N-labelled protease and unlabelled BPTI or *vice versa*. Tagging of the S68C mutant of the protease was performed after formation of the 1:1 complex with BPTI by addition to a 3-fold excess of the C2 tag loaded with either Y^{3+} or Tb^{3+} [35,5]. Following 5 h incubation at room temperature, the complex was washed with NMR buffer using a centrifugal filter unit (Amicon Ultra with a MWCO of 3 kDa; Millipore, Billerica, USA).

2.3. NMR spectroscopy

All NMR spectra were recorded of 0.1–0.2 mM solutions of the protease-BPTI complex in NMR buffer at 25 °C, using a Bruker 800 MHz NMR spectrometer equipped with a TCI cryoprobe. □CSs were measured in ppm as the amide proton chemical shifts measured in the presence of a paramagnetic lanthanide minus the chemical shift observed in the presence of diamagnetic Y^{3+}.

2.4. Δχ-tensor fitting

The PCS of a nuclear spin, $\Delta\delta^{PCS}$, is measured in ppm as the difference in chemical shift between a sample with a paramagnetic ion (Tb^{3+} in the present work) and a sample with a diamagnetic ion. PCSs arise from an anisotropic magnetic susceptibility ($\Delta\chi$) tensor associated with the unpaired electrons of the paramagnetic ion. PCSs follow the equation [36]:

$$\Delta\delta^{PCS} = 1/(12\pi r^3)[\Delta\chi_{ax}(3\cos^2\theta - 1) + 1.5\Delta\chi_{rh}\sin^2\theta\,\square\cos 2\phi] \quad (1)$$

where $\Delta\delta^{PCS}$ is the PCS, r is the distance of the nuclear spin from the metal ion, $\Delta\chi_{ax}$ and $\Delta\chi_{rh}$ are the axial and rhombic components of the $\Delta\chi$ tensor, and θ and ϕ are the polar angles describing the position of the nuclear spin with respect to the principal axes of the $\Delta\chi$ tensor. PCSs from lanthanide tags can be measured for nuclear spins over 40 Å from the metal ion [37].

The PCSs measured for the complex of NS2B-NS3pro with BPTI were used to determine the position and orientation of the magnetic susceptibility anisotropy ($\Delta\chi$) tensors of the paramagnetic ions relative to the protein structure. The program Numbat [38] was used to fit the $\Delta\chi$ tensors to the crystal structure of the complex with BPTI (PDB ID: 3U1J [10]). As no electron density of NS2Bc was observed in the structure 3U1J, the coordinates of NS2Bc in the crystal structure with the peptide inhibitor Bz-nKRR-H (PDB ID: 3U1I [10]) were grafted onto the 3U1J structure for a complete model of the closed conformation.

3. Results

3.1. The complex of the protease with BPTI is stable

Producing the protease as a single polypeptide chain with a self-cleavage site between NS2B and NS3pro ensured a precise 1:1 ratio of both components in the final protease. Cell-free synthesis of BPTI produced correctly folded, selectively ^{15}N-labelled protein (Fig. S1), yielding well-resolved ^{15}N-HSQC cross-peaks that were straightforward to assign to individual residues by comparison with resonance assignments of the free protein (Fig. 2B).

In our hands, samples of the protease without covalent link between NS2B and NS3pro are stable for only a few hours at room temperature in the absence of inhibitor. Sample degradation results in additional narrow cross-peaks from NS2B at random coil chemical shifts which, previously, had erroneously been attributed to open conformations [39,40,5]. Notably, ^{15}N-HSQC spectra of the complex with BPTI were free of these additional cross-peaks and stable for at least a month, indicating that BPTI inhibits the degradation of the protease (Fig. S2).

3.2. The binding mode of BPTI in solution is the same as in the crystal

Fig. 2 illustrates the PCSs observed for the complex of the S68C mutant of the protease with BPTI, with the C2-Tb^{3+} tag ligated to Cys68. The same construct ligated with diamagnetic C2-Y^{3+} served as the diamagnetic reference. PCSs of NS2B-NS3pro were observed in the sample of ^{15}N-labelled protease with unlabelled BPTI (Fig. 2A), while PCSs of BPTI were observed in the sample of selectively ^{15}N-labelled BPTI with unlabelled protease (Fig. 2B). Using the previously established assignment of the protease [5], 21 PCSs could be resolved for NS3pro and residues 55*–65* of NS2B (NS2Bn), and 8 PCSs for NS2Bc. Owing to the better spectral resolution in the selectively ^{15}N-labelled BPTI sample, PCSs could be assigned and accurately measured for 23 residues of the BPTI construct.

To verify that BPTI binds to the protease in solution as reported by the crystal structure 3U1J, we used the PCSs from NS3pro and residues 55*–65* of NS2B to fit an initial $\Delta\chi$ tensor to the crystal structure (Fit 1 in Table 1). The good quality of the fit is illustrated by the close correlation between experimental and back-calculated PCSs (Fig. 3A). Using the fitted $\Delta\chi$ tensor together with the crystal structure coordinates of the DENV-3 protease-BPTI complex (PDB ID: 3U1I [10]) to predict the PCSs of BPTI reproduced the expected trend (Fig. 3C). This shows that the inhibitor binds in solution as reported by the crystal structure (Fig. 3E). This conclusion is unaffected by the observation that the back-calculated PCSs of BPTI were consistently more positive than the experimental PCSs (Fig. 3C). Discrepancies of this magnitude are common for mobile tags like the C2 tag, as translational motions of the metal ion compromise the accuracy with which the PCS data can be approximated by a single effective $\Delta\chi$ tensor [41].

3.3. NS2Bc retains the closed conformation in the presence of BPTI

To obtain more accurate predictions for the PCSs of NS2Bc in the closed conformation, we accepted the correctness of the crystal structure 3U1I [10] with regard to the position of BPTI and determined a new $\Delta\chi$ tensor using amide PCSs of residues from NS3pro, NS2Bn and, in addition, BPTI, so long as they were within 30 Å of the metal ion position determined by Fit 1. The resulting fit (Fit 2 in Table 1) still produced good agreement between back-calculated and experimental PCSs (Fig. 3B) and

accurately predicted the PCSs also for BPTI residues located further than 30 Å from the metal centre (Fig. S3B). Most important, however, the PCSs predicted for NS2Bc in the closed conformation of the crystal structure (3U1I [10]) very closely matched the experimental data (Fig. 3D). This indicates that NS2Bc is in the closed conformation as in the crystal structure with the peptide inhibitor (3U1I [10]) and as determined by NMR in the absence of an inhibitor [7]. Using the PCSs to fit a $\Delta\chi$ tensor to NS2Bn and NS3pro in the open conformation of Fig. 1A (2FOM [4]) predicted completely wrong PCSs for NS2Bc, confirming that this conformation cannot be populated to any significant extent in the complex with BPTI (Fig. S4).

Our results suggest that the open conformation observed in the crystal structure of the protease–BPTI complex could be a crystallization artifact. Indeed, inspection of intermolecular contacts in the crystal lattice show that a symmetry-related molecule occupies much of the space where the β-hairpin of NS2Bc would be expected to be in the closed conformation (Fig. S5).

4. Discussion

The present work demonstrates that the C-terminal β-hairpin of NS2B, NS2Bc, retains the closed conformation in solution also when BPTI is bound to the dengue virus NS2B–NS3 protease. Previous solution NMR data showed that the protease assumes the closed conformation also in the absence of an inhibitor [6,7]. Without exception, the closed conformation thus is the overwhelmingly predominant conformation in solution, regardless of the presence or absence of inhibitors of high or low molecular mass. These results are in stark contrast to the crystal structure determinations of the NS2B-NS3 protease, which reported NS2Bc exclusively in open conformations except for a single case in which a small peptide inhibitor was bound to the protease [4,42,10]. Our results have important implications for rational drug design: while the crystallizations indicate that the association between NS2Bc and NS3pro may be weak, the closed conformation, as observed in the crystal structure with a small peptide inhibitor [10], is the most faithful representation of the protease structure to use in drug development efforts.

Notably, the NS2B-NS3 protease is subject to conformational changes, as indicated by non-uniform peak intensities in the ^{15}N-HSQC spectra (Fig. 2A). High pH (7.5 versus 6.5) or high concentrations of NaCl (300 mM) in the absence of any inhibitor have been observed to broaden the signals of NS2Bc after Ser71* beyond detection, which can be attributed to an equilibrium between open and closed conformations (with residues preceding Ser71* retaining their location in the closed state) or to conformational changes within the closed state [7]. The non-uniform peak intensities in the presence of BPTI indicate that the inhibitor does not eliminate all conformational exchange processes in the protease. As the PCSs of NS2Bc closely match the expectations for the closed conformation and we could not observe signals of an additional conformation, we estimate that at most 10% of NS2Bc in an open conformation could have escaped detection.

On a technical note, our data illustrate the power of pseudocontact shifts for the structure analysis of proteins and protein-ligand complexes in aqueous solution, even if the lanthanide tag is attached via a fairly flexible linker. An earlier analysis of the C1 tag (which is the opposite enantiomer of the C2 tag used here) attached to the NS2B–NS3 protease concluded that the mobility of the tag can compromise the prediction of accurate PCSs of a ligand, if a single effective $\Delta\chi$ tensor is fitted to all experimental PCS data of the protein [41]. This effect arises from the fact that, in principle, displacements of the metal requires the fitting of multiple $\Delta\chi$ tensors for accurate PCS back-calculations. Much improved PCS predictions are already expected, however, if a single effective $\Delta\chi$ tensor is fitted to a subset of PCSs measured for nuclear spins in the vicinity of the ligand. This expectation is borne out by the experimental data of the present work, as the PCSs predicted for NS2Bc matched the experimental results much better, when PCSs from nuclear spins of BPTI were included to fit the $\Delta\chi$ tensor while excluding those BPTI amides that were located far from the metal site. In this way, the approximation of the PCS data by a single effective $\Delta\chi$ tensor resulted in a good fit of PCSs for nuclear spins in the vicinity of NS2Bc (Fig. 3F), producing a meaningful prediction of PCSs for NS2Bc and comparison with experimental PCSs.

In conclusion, our results stress the stability of the closed conformation of the dengue virus NS2B–NS3 protease, at least for serotype 2 which is the serotype with the

highest global growth rate over the last decade [43]. NMR studies of the other serotypes will be required to assess the effect of sequence differences on the prevalence of open conformations. Our results also highlight the way in which PCSs induced by fairly mobile lanthanide tags can be used to obtain useful structural information in solution for protein systems that are difficult to analyse in detail by conventional techniques.

5. Author contributions

W.N.C., K.L. and G.O. designed experiments. K.L., C.N. and B.G. generated reagents. W.N.C. performed experiments. W.N.C. and G.O. wrote and edited the manuscript.

Acknowledgements

We thank Prof. Takanori Kigawa for the expression constructs of BPTI and DsbC. W.-N. C. thanks the government of the People's Republic of China for a CSC scholarship and C.N. thanks the Studienstiftung des deutschen Volkes for a fellowship. Financial support by the Australian Research Council is gratefully acknowledged.

References

[1] Bhatt, S., Gething, P.W., Brady, O.J., Messina, J.P., Farlow, A.W., Moyes, C.L., Drake, J.M., Brownstein, J.S., Hoen, A.G., Sankoh, O., Myers, M.F., George, D.B., Jaenisch, T., Wint, G.R., Simmons, C.P., Scott, T.W., Farrar, J.J. and Hay, S.I. (2013) The global distribution and burden of dengue. Nature 496, 504–507.

[2] Lescar, J., Luo, D., Xu, T., Sampath, A., Lim, S.P., Canard, B. and Vasudevan, S.G. (2008) Towards the design of antiviral inhibitors against flaviviruses: the case for the multifunctional NS3 protein from Dengue virus as a target. Antiviral Res. 80, 94–101.

[3] Rothan, H.A., Han, H.C., Ramasamy, T.S., Othman, S., Rahman, N.A. and Yusof, R. (2012) Inhibition of dengue NS2B-NS3 protease and viral replication in Vero cells by recombinant retrocyclin-1. BMC Infect. Dis. 12, 314.

[4] Erbel, P., Schiering, N., D'Arcy, A., Renatus, M., Kroemer, M., Lim, S. P., Yin, Z., Keller, T.H., Vasudevan, S.G. and Hommel, U. (2006) Structural basis for the activation of flaviviral NS3 proteases from dengue and West Nile virus. Nat. Struct. Mol. Biol. 13, 372–373.

[5] de la Cruz, L., Nguyen, T.H., Ozawa, K., Shin, J., Graham, B., Huber, T. and Otting, G. (2011) Binding of low molecular weight inhibitors promotes large conformational changes in the dengue virus NS2B-NS3 protease: fold analysis by pseudocontact shifts. J. Am. Chem. Soc. 133, 19205–19215.

[6] Kim, Y.M., Gayen, S., Kang, C., Joy, J., Huang, Q., Chen, A.S., Wee, J.L., Ang, M.J., Lim, H.A., Hung, A.W., Li, R., Noble, C.G., Lee, L.T., Yip, A., Wang, Q.Y., Chia, C.S., Hill, J., Shi, P.Y. and Keller, T.H. (2013) NMR analysis of a novel enzymatically active unlinked dengue NS2B-NS3 protease complex. J. Biol. Chem. 288, 12891–12900.

[7] de la Cruz, L., Chen, W.N., Graham, B. and Otting, G. (2014) Binding mode of the activity-modulating C-terminal segment of NS2B to NS3 in the dengue virus NS2B-NS3 protease. FEBS J. 281, 1517–1533.

[8] Aleshin, A.E., Shiryaev, S.A., Strongin, A.Y. and Liddington, R.C. (2007) Structural evidence for regulation and specificity of flaviviral proteases and evolution of the Flaviviridae fold. Protein Sci. 16, 795–806.

[9] Robin, G., Chappell, K., Stoermer, M.J., Hu, S., Young, P.R., Fairlie, D.P. and Martin, J.L. (2009) Structure of West Nile virus NS3 protease: ligand stabilization of the catalytic conformation. J. Mol. Biol. 385, 1568–1577.

[10] Noble, C.G., Seh, C.C., Chao, A.T. and Shi, P.Y. (2012) Ligand-bound structures of the dengue virus protease reveal the active conformation. J. Virol. 86, 438–446.

[11] Mueller, N.H., Yon, C., Ganesh, V.K. and Padmanabhan, R. (2007) Characterization of the West Nile virus protease substrate specificity and inhibitors. Int. J. Biochem. Cell Biol. 39, 606–614.

[12] Yin, Z., Patel, S.J., Wang, W.L., Chan, W.L., Rao, K.R.R., Wang, G., Ngew, X., Patel, V., Beer, D., Knox, J.E., Ma, N.L., Ehrhardt, C., Lim, S.P., Vasudevan, S.G. and Keller, T.H. (2006) Peptide inhibitors of dengue virus NS3 protease. Part 2: SAR study of tetrapeptide aldehyde inhibitors. Bioorg. Med. Chem. Lett. 16, 40–43.

[13] Tomlinson, S.M. and Watowich, S.J. (2011) Anthracene-based inhibitors of dengue virus NS2B-NS3 protease. Antiviral Res. 89, 127–135.

[14] Knehans, T., Schüller, A., Doan, D.N., Nacro, K., Hill, J., Güntert, P., Madhusudhan, M.S., Weil, T. and Vasudevan, S.G. (2011) Structure-guided fragment-based *in silico* drug design of dengue protease inhibitors. J. Comput. Aided Mol. Des. 25, 263–274.

[15] Schüller, A., Yin, Z., Chia, C.S.B., Doan, D.N., Kim, H.K., Shang, L., Loh, T.P., Hill, J. and Vasudevan, S.G. (2011) Tripeptide inhibitors of dengue and West Nile virus NS2B-NS3 protease. Antiviral Res. 92, 96–101.

[16] Doan, D.N., Li, K.Q., Basavannacharya, C., Vasudevan, S.G. and Madhusudhan, M.S. (2012) Transplantation of a hydrogen bonding network from West Nile virus protease onto dengue-2 protease improves catalytic efficiency and sheds light on substrate specificity. Protein Eng. Des. Sel. 25, 843–850.

[17] Xu, S., Li, H., Shao, X., Fan, C., Ericksen, B., Liu, J., Chi, C. and Wang, C. (2012) Critical effect of peptide cyclization on the potency of peptide inhibitors against dengue virus NS2B-NS3 protease. J. Med. Chem. 55, 6881–6887.

[18] Ghanesh, V.K., Muller, N., Judge, K., Luan, C.H., Padmanabhan, R. and Murthy, K.H.M. (2005) Identification and characterization of nonsubstrate based inhibitors of the essential dengue and West Nile virus proteases. Bioorg. Med. Chem. 13, 257–264.

[19] Frecer, V. and Miertus, S. (2010) Design, structure-based focusing and *in silico* screening of combinatorial library of peptidomimetic inhibitors of Dengue virus NS2B-NS3 protease. J. Comput. Aided Mol. Des. 24, 195–212.

[20] Tambunan, U.S.F. and Alamudi, S. (2010) Designing cyclic peptide inhibitor of dengue virus NS3-NS2B protease by using molecular docking approach. Bioinformation 5, 250–254.

[21] Frimayanti, N., Chee, C.F., Zain, S.M. and Rahman, N.A. (2011) Design of new competitive dengue Ns2b/Ns3 protease inhibitors – a computational approach. Int. J. Mol. Sci. 12, 1089–1100.

[22] Lai, H., Prasad, G.S., Padmanabhan, R. (2013) Characterization of 8-hydroxyquinoline derivatives containing aminobenzothiazole as inhibitors of dengue virus type 2 protease *in vitro*. Antivir. Res. 97, 74–80.

[23] Prusis, P., Junaid, M., Petrovska, R., Yahorava, S., Yahorau, A., Katzenmeier, G., Lapins, M. and Wikberg, J.E. (2013) Design and evaluation of substrate-based octapeptide and non substrate-based tetrapeptide inhibitors of dengue virus NS2B-NS3 proteases. Biochem. Biophys. Res. Commun. 434, 767–772.

[24] Wichapong, K., Nueangaudom, A., Pianwanit, S., Sippl, W. and Kokpol, S. (2013) Identification of potential hit compounds for Dengue virus NS2B/NS3 protease inhibitors by combining virtual screening and binding free energy calculations. Trop. Biomed. 30, 388–408.

[25] Nitsche, C., Schreier, V.N., Behnam, M.A., Kumar, A., Bartenschlager, R. and Klein, C.D. (2013) Thiazolidinone-peptide hybrids as dengue virus protease inhibitors with antiviral activity in cell culture. J. Med. Chem. 56, 8389–8403.

[26] Pambudi, S., Kawashita, N., Phanthanawiboon, S., Omokoko, M.D., Masrinoul, P., Yamashita, A., Limkittikul, K., Yasunaga, T., Takagi, T., Ikuta, K. and Kurosu, T. (2013) A small compound targeting the interaction between nonstructural proteins 2B and 3 inhibits dengue virus replication. Biochem. Biophys. Res. Commun. 440, 393–398.

[27] Yildiz, M., Ghosh, S., Bell, J.A., Sherman, W. and Hardy, J.A. (2013) Allosteric inhibition of the NS2B-NS3 protease from dengue virus. ACS Chem. Biol. 8, 2744–2742.

[28] Zhou, G.C., Weng, Z., Shao, X., Liu, F., Nie, X., Liu, J., Wang, D., Wang, C. and Guo, K. (2013) Discovery and SAR studies of methionine-proline anilides as dengue virus NS2B-NS3 protease inhibitors. Bioorg. Med. Chem. Lett. 23, 6549–6554.

[29] Neylon, C., Brown, S.E., Kralicek, A.V., Miles, C.S., Love, C.A. and Dixon, N.E. (2000) Interaction of the *Escherichia coli* replication terminator protein (Tus) with DNA: a model derived from DNA-binding studies of mutant proteins by surface

plasmon resonance. Biochemistry 39, 11989–11999.

[30] Matsuda, T., Watanabe, S. and Kigawa, T. (2013) Cell-free synthesis system suitable for disulfide-containing proteins. Biochem. Biophys. Res. Commun. 431, 296–301.

[31] Sivashanmugam, A., Murray, V., Cui, C.X., Zhang, Y.H., Wang, J.J. and Li, Q.Q. (2009) Practical protocols for production of very high yields of recombinant proteins using *Escherichia coli*. Protein Sci. 18, 936–948.

[32] Ozawa, K., Headlam, M.J., Schaeffer, P.M., Henderson, B.R., Dixon, N.E. and Otting, G. (2004) Optimization of an *Escherichia coli* system for cell-free synthesis of selectively ^{15}N-labelled proteins for rapid analysis by NMR spectroscopy. Eur. J. Biochem. 271, 4084–4093.

[33] Apponyi, M.A., Ozawa, K., Dixon, N.E. and Otting, G. (2008) Cell-free protein synthesis for analysis by NMR spectroscopy. Methods Mol. Biol. 426, 257–268.

[34] Jia, X., Ozawa, K., Loscha, K. and Otting, G. (2009) Glutarate and N-acetyl-L-glutamate buffers for cell-free synthesis of selectively ^{15}N-labelled proteins. J. Biomol. NMR 44, 59–67.

[35] Graham, B., Loh, C.T., Swarbrick, J.D., Ung, P., Shin, J., Yagi, H., Jia, X., Chhabra, S., Barlow, N., Pintacuda, G., Huber, T. and Otting, G. (2011) DOTA-amide lanthanide tag for reliable generation of pseudocontact shifts in protein NMR spectra. Bioconjugate Chem. 22, 2118–2125.

[36] Bertini, I., Luchinat, C. and Parigi, G. (2002) Magnetic susceptibility in paramagnetic NMR. Prog. NMR Spectr. 40, 249–273.

[37] Otting, G. (2008) Prospects for lanthanides in structural biology by NMR. J. Biomol. NMR 42, 1–9.

[38] Schmitz, C., Stanton-Cook, M.J., Su, X.C., Otting, G. and Huber, T. (2008) Numbat: an interactive software tool for fitting $\Delta\chi$ to molecular coordinates using pseudocontact shifts. J. Biomol. NMR 41, 179–189.

[39] Wu, P.S.C., Ozawa, K., Lim, S.P., Vasudevan, S.G., Dixon, N.E. and Otting, G. (2007) Cell-free transcription/translation from PCR-amplified DNA for high-throughput NMR studies. Angew. Chemie Int. Ed. 46, 3356–3358.

[40] Su, X.C., Ozawa, K., Qi, R., Vasudevan, S.G., Lim, S.P. and Otting, G. (2009) NMR analysis of the dynamic exchange of the NS2B cofactor between open and closed

conformations of the West Nile virus NS2B-NS3 protease. PLoS Negl. Trop. Dis. 3, e561.

[41] Shishmarev, D. and Otting, G. (2013) How reliable are pseudocontact shifts induced in proteins and ligands by mobile paramagnetic metal tags? A modelling study. J. Biomol. NMR 56, 203–216.

[42] Chandramouli, S., Joseph, J.S., Daudenarde, S., Gatchalian, J., Cornillez-Ty, C. and Kuhn, P. (2010) Serotype-specific structural differences in the protease-cofactor complexes of the dengue virus family. J. Virol. 84, 3059–3067.

[43] Costa, R.L., Voloch, C.M. and Schrago, C.G. (2012) Comparative evolutionary epidemiology of dengue virus serotypes. Infect. Genet. Evol. 12, 309–314.

Table 1. Δχ-tensor parameters of the protease–BPTI complex with the C2-Tb^{3+} tag attached to residue 68 of NS3pro[a]

	$\Delta\chi_{ax}$	$\Delta\chi_{rh}$	x	y	z	α	β	γ
Fit 1[b]	-12.3	-4.0	-16.098	-34.428	3.681	146.1	48.9	30.1
	(0.1)	(0.6)	(0.3)	(0.3)	(0.2)	(2.5)	(1.2)	(4.7)
Fit 2[c]	-12.9	-1.9	-16.800	-33.423	3.582	144.0	50.9	67.7
	(0.2)	(0.3)	(0.1)	(0.3)	(0.1)	(1.5)	(0.6)	(3.1)

[a] Δχ-tensor parameters determined by the program Numbat using the crystal structure 3U1J. The axial and rhombic components of the Δχ tensors are given in 10^{-32} m^3 and the Euler angles in degrees, using the zyz convention and unique tensor representation [38]. Uncertainties (in brackets) were estimated by randomly omitting 10% of the PCS data in multiple tensor fits.

[b] Fit 1 used only PCSs from NS3pro and residues 55*–65* of NS2B. The root mean square deviation (rmsd) between the experimental and back-calculated PCSs was 0.014 ppm for the residues included in the fit.

[c] Fit 2 used only PCSs from NS3pro, residues 55*–65* of NS2B, and PCSs from those BPTI amides, which are within 30 Å from the paramagnetic metal centre determined by Fit 1. The rmsd between the experimental and back-calculated PCSs was 0.029 ppm for the residues included in the fit.

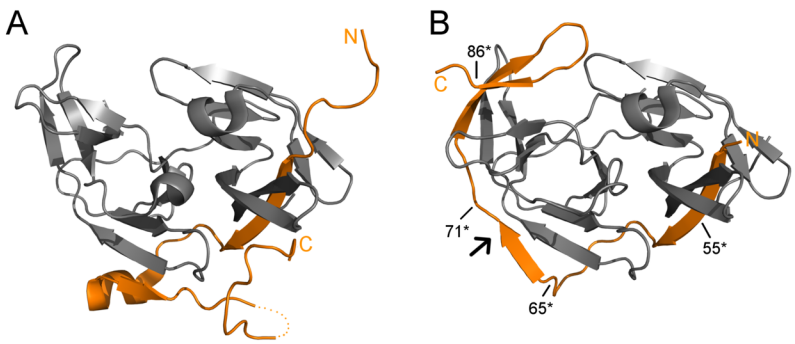

Fig. 1. Ribbon drawings of the dengue virus NS2B-NS3 protease as observed in crystal structures. NS3pro is shown in grey and NS2B in orange. The active site is located near the centre top in the orientation shown. The N-terminal segment of NS2B (NS2Bn, residues 55*–65*) forms a structurally conserved β-strand that inserts into the N-terminal β-barrel of NS3pro. The C-terminal segment of NS2B (NS2Bc, residues 66*–95*) differs greatly between the open (panel A, PDB ID: 2FOM) and closed (panel B, PDB ID: 3U1I [10]) conformations detected by X-ray crystallography [4,10]. The arrow identifies the last residue of NS2B, for which electron density was observed in the complex with BPTI (PDB ID: 3U1J [10]). The positions of selected residues are indicated.

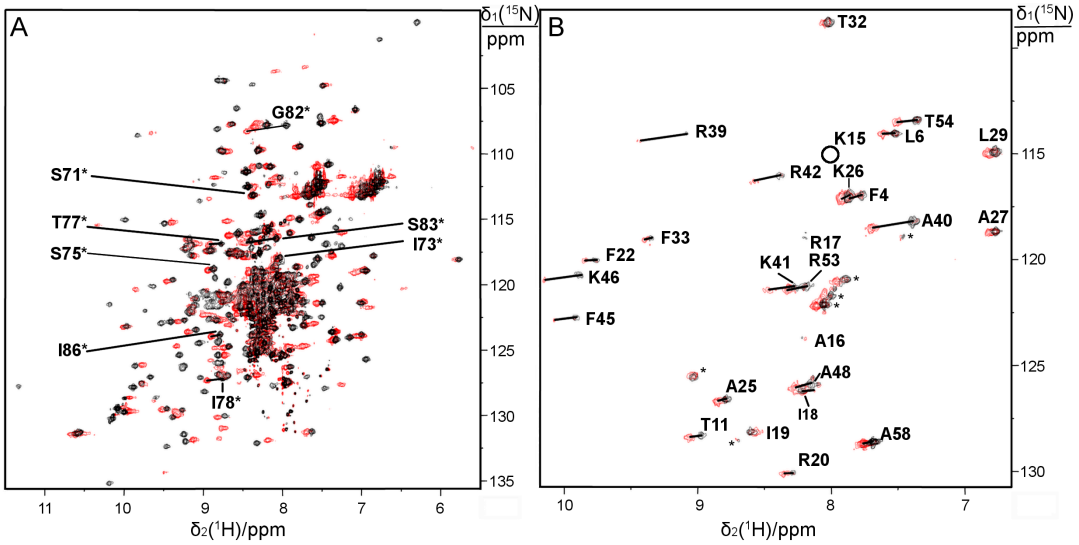

Fig. 2. PCSs observed for the complex of NS2B-NS3 protease with BPTI. (A) Superimposition of ^{15}N-HSQC spectra of uniformly ^{15}N-labelled protease S68C, tagged with either C2-Tb^{3+} (red spectrum) or C2-Y^{3+} (black spectrum), in complex with unlabelled BPTI. PCSs of NS2Bc residues are labelled. (B) Same as (A), except that the protease is at natural isotopic abundance and BPTI is selectively labelled with ^{15}N-Ala, Arg, Lys, Thr, Leu, Phe and Ile. PCSs of BPTI are identified by lines. Cross-peaks of residues 15 (circle) and 17 were observable only at the noise level. Asterisks identify unassigned resonances attributed to the modified N-terminus and the nearby C-terminus.

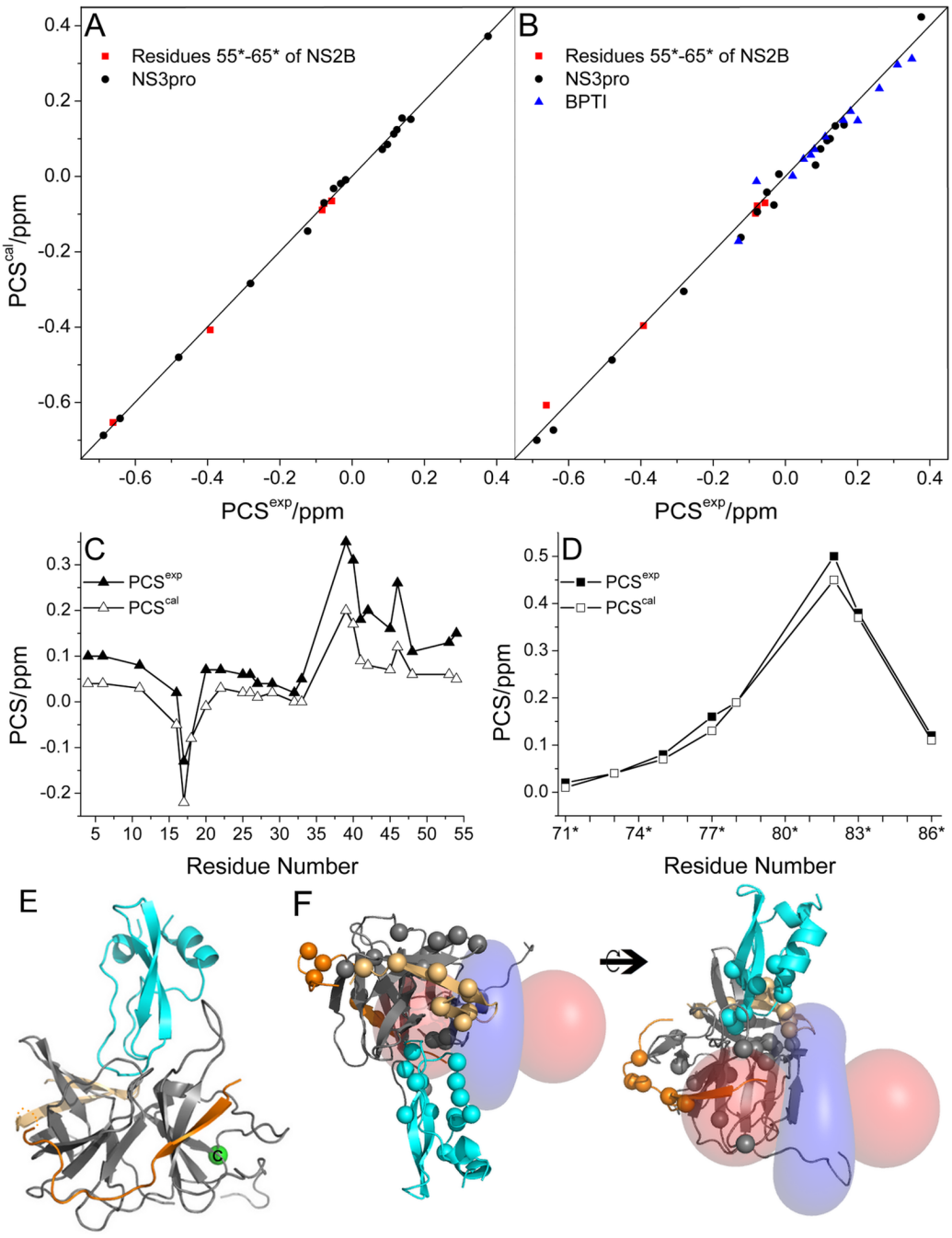

Fig. 3. Correlation between experimental and calculated PCSs for the complex of NS2B-NS3pro with BPTI. (A) Back-calculated versus experimental PCSs produced by Fit 1 of Table 1. Data of NS2B (residues 55*–65*) and NS3pro are shown as red squares and black circles, respectively. (B) Same as (A), except showing the data from Fit 2. PCSs from BPTI are shown as blue triangles. (C) PCSs of BPTI predicted by the Δχ tensor of

Fit 1 versus the amino-acid sequence of BPTI. Experimental and calculated data are shown as black and white triangles, respectively. (D) PCSs of NS2Bc predicted by the $\Delta\chi$ tensor of Fit 2 versus the amino-acid sequence of NS2Bc. Experimental and calculated data are shown as black and white squares, respectively. (E) Cartoon representation of the structure 3U1J with NS2Bc copied from the structure 3U1I [10]. The N-terminal segment of NS2B is shown in orange, NS2Bc in light orange, NS3pro in grey and BPTI in cyan. The link between residues 69* and 70* is indicated by dots. The green sphere highlights the site of the cysteine residue carrying the lanthanide tag (residue 68). (F) PCS isosurfaces (± 0.5 ppm) generated by the $\Delta\chi$ tensor of Fit 2 (Table 1) plotted on the structure of the protease–BPTI complex. Blue and red surfaces identify, respectively, positive and negative PCSs. The amides for which PCSs were measured and used in the fit are identified by spheres. Light orange balls illustrate amides of NS2Bc for which experimental PCSs were measured. The same data are displayed in two different orientations.